Reactivity of Sulfenic Acid in Human Serum Albumin†

Lucía Turell,[‡,§,||] Horacio Botti,[||,⊥] Sebastián Carballal,[‡,||,⊥] Gerardo Ferrer-Sueta,[§,||] José M. Souza,[||,⊥] Rosario Durán,[#] Bruce A. Freeman,[▽] Rafael Radi,[||,⊥] and Beatriz Alvarez*[,‡,||]

Laboratorios Enzimología and Fisicoquímica Biológica, Facultad de Ciencias, and Center for Free Radical and Biomedical Research and Departamento de Bioquímica, Facultad de Medicina, Universidad de la República, and Instituto de Investigaciones Biológicas Clemente Estable and Institut Pasteur de Montevideo, Montevideo, Uruguay, and Department of Pharmacology, University of Pittsburgh Medical Center, Pittsburgh, Pennsylvania

Received July 30, 2007; Revised Manuscript Received October 25, 2007

ABSTRACT: Sulfenic acid is formed upon oxidation of thiols and is a central intermediate in the redox modulation of an increasing number of proteins. Methods for quantifying or even detecting sulfenic acid are scarce. Herein, the reagent 7-chloro-4-nitrobenz-2-oxa-1,3-diazole was determined not to be suitable as a chromophoric probe for sulfenic acid in human serum albumin (HSA−SOH) because of lack of specificity. Thionitrobenzoate (TNB) reacted with HSA exposed to hydrogen peroxide, but not control or thiol-blocked HSA. The reaction was biphasic. The first phase was ∼20-fold faster than the second phase and first order in HSA−SOH and TNB (105 ± 11 M^{-1} s^{-1}, 25 °C, pH 7.4), allowing quantitative data on HSA−SOH formation and reactivity to be obtained. Exposure of reduced HSA (0.5 mM) to hydrogen peroxide (4 mM, 37 °C, 4 min) yielded 0.18 ± 0.02 mol of HSA−SOH per mol of HSA. HSA−SH reacted with hydrogen peroxide at 2.7 ± 0.7 M^{-1} s^{-1} (37 °C, pH 7.4), while HSA−SOH reacted at 0.4 ± 0.2 M^{-1} s^{-1}, yielding sulfinic acid (HSA−SO_2H), as detected by mass spectrometry. The rate constants of HSA−SOH with targets of analytical interest such as dimedone and sodium arsenite were determined. HSA−SOH did not react appreciably with the plasma reductants ascorbate or urate, nor with free basic amino acids. In contrast, HSA−SOH reacted rapidly with the plasma thiols cysteine, glutathione, homocysteine, and cysteinylglycine at 21.6 ± 0.2, 2.9 ± 0.5, 9.3 ± 0.9, and 55 ± 3 M^{-1} s^{-1} (25 °C, pH 7.4), respectively, supporting a role for HSA−SOH in the formation of mixed disulfides.

Reactive oxygen species are produced by aerobic metabolism and at elevated rates in diverse pathophysiological conditions. Proteins are preferential targets for reactive oxygen species, and cysteine (Cys)[1] residues are particularly susceptible to oxidation. With one- and two-electron reduction potentials of $E^{\circ\prime}$(CysS•/CysSH) = 0.92 V and $E^{\circ\prime}$-(CysSSCys/CysSH) = −0.24 V (*1*, *2*), cysteine can be oxidized by a wide spectrum of oxidant species. Cysteine oxidation modulates signaling mechanisms, coupling changes in the redox state to cellular processes (*3*, *4*). Among the different oxidation products, sulfenic acid (RSOH) has been identified in a growing list of redox-susceptible proteins where it serves catalytic or regulatory functions (*5*, *6*).

Sulfenic acid is mainly formed after the two-electron oxidation of a thiol with oxidants such as hydrogen peroxide and peroxynitrite (*7*) and exhibits both nucleophilic and electrophilic reactivity. Consequently, it can react with a thiol, leading to a disulfide, or condense with another sulfenic acid to form a thiosulfinate (RS(O)SR) (*5*, *8*, *9*). Due to its high reactivity, sulfenic acid was considered a transient intermediate in the oxidation of thiols. However, stabilized sulfenic acids have been identified recently in several proteins, where the absence of proximal thiols is the main factor to account for stabilization (*6*, *10*).

Sulfenic acid does not possess distinguishing UV−vis absorbance or fluorescence features; thus, different tools and chemical methods have been developed for trapping and identifying this functional group. Since there are few electrophilic groups in proteins, the fact that nucleophiles can react with the sulfur atom of sulfenic acid can be used for its detection. The nucleophilic reagent dimedone (5,5-

† This work was supported by grants from the Programa de Desarrollo Tecnológico-II (Ministry of Education and Culture, Uruguay), Philip Morris USA Inc., Philip Morris International, the NIH (HL58115, HL64937) and the Howard Hughes Medical Institute. R.R. is a Howard Hughes International Research Scholar.

* To whom correspondence should be addressed. Phone: +598-2-5258618. Fax: +598-2-5250749. E-mail: beatriz.alvarez@fcien.edu.uy.

‡ Laboratorio de Enzimología, Facultad de Ciencias, Universidad de la República.

§ Laboratorio de Fisicoquímica Biológica, Facultad de Ciencias, Universidad de la República

|| Center for Free Radical and Biomedical Research, Facultad de Medicina, Universidad de la República.

⊥ Departamento de Bioquímica, Facultad de Medicina, Universidad de la República.

Instituto de Investigaciones Biológicas Clemente Estable and Institut Pasteur de Montevideo.

▽ University of Pittsburgh Medical Center.

[1] Abbreviations: HSA, human serum albumin, HSA−SH, thiol of human serum albumin; HSA−SH/HSA, mol of thiol per mol of HSA; HSA−SOH, sulfenic acid in human serum albumin; HSA−SOH/HSA, mol of sulfenic acid per mol of HSA; DTNB, 5,5′-dithiobis(2-nitrobenzoate); TNB, thionitrobenzoate; NEM, *N*-ethylmaleimide; NBD−Cl, 7-chloro-4-nitrobenz-2-oxa-1,3-diazole; dimedone, 5,5-dimethyl-1,3-cyclohexanedione; DTPA, diethylenetriaminepentaacetic acid; *p*-CMB, *p*-chloromercuribenzoate; DTT, dithiothreitol; Cys, cysteine; Hcy, homocysteine; GSH, glutathione; CysGly, cysteinylglycine; MS, mass spectrometry; ESI, electrospray ionization; MALDI-TOF, matrix-assisted laser desorption ionization time of flight.

10.1021/bi701520y CCC: $40.75
Published on Web 12/14/2007

dimethyl-1,3-cyclohexanedione) reacts specifically with sulfenic acid to form a stable thioether adduct (*11*) which can be identified by mass spectrometry or using radioactively labeled compounds. Recently, modified dimedones have been designed that yield fluorescent or biotinylated products (*12*, *13*). Sulfenic acid can also be determined using thionitrobenzoate (TNB), another nucleophilic reagent that forms mixed disulfides and results in a loss in the absorbance at 412 nm (*14*−*17*). The electrophilic reagent 7-chloro-4-nitrobenz-2-oxa-1,3-diazole (NBD−Cl) has also been employed to detect sulfenic acid in several proteins including HSA (*18*−*22*). Finally, sulfenic acid can be detected after its reaction with arsenite, since arsenite reduces sulfenic acid back to the thiol but does not reduce disulfides. Arsenite has been used in proteomic studies (*23*). However, suitable approaches for obtaining quantitative and kinetic data are scarce; hence, information regarding the properties and reactivity of biological sulfenic acid is limited.

Human serum albumin (HSA) is the most abundant protein in plasma (0.6 mM), representing ∼60% of the total protein. Among its 585 amino acids it contains 35 cysteines, 34 of which form disulfide bonds, leaving one free cysteine, Cys34 (*24*). About 70% of circulating HSA contains this Cys34 in the reduced state and is known as mercaptalbumin. The nonmercaptalbumin fraction contains mostly mixed disulfides with cysteine and other low molecular weight thiols, while a significant amount is oxidized to higher oxidation states such as sulfinic and sulfonic acids (HSA−SO_2H and HSA−SO_3H). The HSA thiol (HSA−SH) is the preferential plasma target of the reactive species generated by xanthine oxidase, which include superoxide, hydrogen peroxide, and hydroxyl radical (*25*). Oxidation most likely implied the formation of sulfenic acid (HSA−SOH), because it reverted with thiol reductants and no intermolecular disulfides were formed. Mass spectral analysis provided definitive evidence for the formation of a sulfenic acid (*22*). HSA−SH reacts with hydrogen peroxide and peroxynitrite with rate constants of 2.26 and 3.8 × 10^3 M^{-1} s^{-1} (37 °C, pH 7.4), respectively (*22*, *26*). Although this thiol does not react particularly fast with oxidants compared, for example, to peroxiredoxins, it remains an important scavenger of intravascular reactive species due to its high plasma concentration (0.4−0.5 mM). In fact, oxidized forms of HSA have been found increased in several pathological conditions (*27*−*30*), and HSA−SOH could be an intermediate in their formation (*22*).

Characterizing the formation and properties of sulfenic acid in a protein such as HSA is complicated by HSA being a large multidomain protein that binds different ligands, some of them allosterically (*24*). In addition, HSA contains 17 disulfide bridges with at least 1 accessible (*31*) and presents pH-dependent structural transitions (*24*). We developed a strategy for quantifying HSA−SOH on the basis of its reaction with the chromophoric thiol TNB and determined the reactivity of HSA−SOH with targets of analytical and biological interest.

EXPERIMENTAL PROCEDURES

Materials. HSA was from ZLB Bioplasma, Switzerland. These HSA preparations intended for clinical use typically contain ∼0.2 HSA−SH/HSA. Hydrogen peroxide was from J. T. Baker, sequencing grade trypsin was from Promega, the Micro Bio-Spin chromatography columns were from Bio-Rad, and the Q-Sepharose fast flow resin and PD-10 gel filtration columns were from Amersham-General Electric Healthcare. The remaining reagents were from Sigma. Absorbance determinations were made in a Shimadzu UV-1603 or a Varian Cary 50 spectrophotometer. An Applied Photophysics RX2000 rapid kinetics accessory was used for stopped flow experiments.

Solutions. All assays, unless specified, were performed in 0.1 M phosphate buffer, pH 7.4, containing 0.1 mM diethylenetriaminepentaacetic acid (DTPA). Hydrogen peroxide solutions were prepared in nanopure water, and their concentration was determined spectrophotometrically at 240 nm (ϵ = 43.6 M^{-1} cm^{-1}) (*32*). Catalase solutions were prepared in phosphate buffer, and the apparent first-order rate constant at 10 mM hydrogen peroxide was determined to estimate their concentration (*33*). NBD−Cl (100 mM) was prepared in dimethyl sulfoxide, dimedone (1 M) in 95% ethanol, and *p*-nitrophenyl acetate (100 mM) in acetonitrile. Ascorbate (0.5 M) and sodium arsenite (0.2 M) were prepared in phosphate buffer, and the pH was adjusted to 7.4. Urate (0.05 M) was prepared in NaOH (0.3 M). L-Alanine, L-histidine, L-lysine, L-arginine, L-cysteine, glutathione, and cysteinylglycine were prepared in nanopure water. Homocysteine was prepared from DL-homocysteine thiolactone by incubation with NaOH (5 M) for 5 min at 37 °C followed by neutralization with HCl (5 M) and phosphate buffer (0.2 M, pH 7.4). Thiol solutions were purged with N_2 for ∼5 min to avoid oxidation, and the thiol concentration was determined with 5,5′-dithiobis(2-nitrobenzoate) (DTNB) before and after the experiment. DTNB for thiol measurements was prepared in pyrophospate buffer (0.1 M, pH 9).

HSA Solutions. HSA was delipidated with activated charcoal (*34*), and its thiol was reduced by overnight incubation with 2-mercaptoethanol (10 mM) at 4 °C. Excess reductant was removed by gel filtration on PD-10 columns equilibrated with phosphate buffer. The HSA concentration was determined from the absorbance at 279 nm (ϵ = 0.531 $(g/L)^{-1}$ cm^{-1}) assuming a molecular mass of 66486 Da (*24*, *35*). Reduced HSA solutions thus prepared had a concentration of ∼1 mM and typically 0.65−0.86 HSA−SH/HSA. The HSA thiol was blocked by incubation with a 7-fold excess of NEM or equimolar $HgCl_2$ for 30 min at room temperature followed by gel filtration.

Oxidation of HSA. To obtain HSA−SOH, reduced HSA (0.5 mM) was incubated with 4 mM hydrogen peroxide for 4 min at 37 °C in phosphate buffer (0.1 M, pH 7.4, 0.1 mM DTPA). Reactions were stopped by the addition of enough catalase to consume 90% of the hydrogen peroxide in 1 s. The solutions thus prepared were maintained on ice, used without further purification, and called "oxidized HSA".

Thiol Determination. In reduced HSA, thiols were measured with DTNB after incubation with excess reagent in sodium pyrophosphate buffer (0.1 M, pH 9) for 5 min in the dark. An absorption coefficient at 412 nm of 14 150 M^{-1} cm^{-1} (*36*) was used to quantify the TNB formed. Because TNB reacts with HSA−SOH, when HSA was previously oxidized, thiols were determined with *p*-chloromercuribenzoate (*p*-CMB) (*37*, *38*). Briefly, HSA (30 μM) was titrated by adding aliquots of *p*-CMB in Tris buffer (0.1 M, pH 7.5) and recording the increase in absorbance at 250 nm.

Product Formation with NBD−Cl and Esterase-like Activity. NBD−Cl (0.4−10 mM) was added to HSA (0.5 mM), incubated for 30 min at 37 °C, and subjected to gel filtration. UV−vis spectra were obtained for reduced, oxidized, and thiol-blocked HSA. The esterase-like activity of HSA was determined by mixing *p*-nitrophenyl acetate (5 μM) with HSA (25 μM) and following the appearance of *p*-nitrophenol at 400 nm (*39*, *40*).

TNB Synthesis and Purification. Solutions of TNB, free of DTNB, were prepared by reduction with 2-mercaptoethanol followed by ion exchange chromatography. Briefly, DTNB (5 mM) was prepared in water, alkalinized until complete dissolution, and incubated with a 20-fold excess of 2-mercaptoethanol for 30 min at room temperature; a 100% yield of TNB was obtained. To remove the remaining 2-mercaptoethanol, the sample was applied to an ion exchange chromatography column (Q-Sepharose fast flow) equilibrated with Tris buffer (pH 7.5, 20 mM). The column was washed with the same buffer and then with water. To elute TNB from the column, HCl (50 mM) was used. The acidic TNB solution was aliquoted and stored at −20 °C. Absence of DTNB from the TNB solutions was confirmed before each experiment by the lack of absorbance increase at 412 nm after addition of glutathione, 2-mercaptoethanol, or reduced HSA.

Reaction between HSA−SOH and TNB. Oxidized HSA (50 μM) was incubated with TNB (70 μM), and the absorbance at 412 nm was recorded at 25 °C. Since the yield of HSA−SOH was ∼18%, this TNB concentration represented a pseudo-first-order excess. Controls with reduced and thiol-blocked HSA and without HSA were included.

Reaction of HSA−SH and HSA−SOH with Hydrogen Peroxide. Reduced HSA (0.5 mM) was incubated with hydrogen peroxide (4 mM) at 37 °C. At increasing times, aliquots (50 μM) were mixed with catalase and TNB (70 μM) previously equilibrated at 25 °C. The absorbance at 412 nm was recorded for 30 s, and the initial rate of the absorbance decrease was determined to evaluate the HSA−SOH concentration.

Reaction of HSA−SOH with Dimedone, Sodium Arsenite, Urate, and Ascorbate. Oxidized HSA (0.5 mM) was incubated at 37 °C in the absence or presence of sodium arsenite (8.7−30 mM), dimedone (90−167 mM), urate (1 mM), or ascorbate (20 mM). At increasing times, aliquots (50 μM) were mixed with TNB (70 μM) previously equilibrated at 25 °C, and the absorbance at 412 nm was recorded for 30 s. The time-dependent decrease in the initial rate was fitted to a single-exponential plus offset equation to determine the pseudo-first-order rate constant k_{obs} at each reagent concentration. Second-order rate constants were determined from k_{obs} versus concentration plots.

Reaction of HSA−SOH with thiols and amines. The rate constants of the reactions of HSA−SOH with thiols were determined using a competition approach with TNB. Oxidized HSA (50 μM) was mixed with TNB (70 μM) in the absence or presence of increasing concentrations of cysteine (0.2−1 mM), glutathione (1−7 mM), homocysteine (1−5 mM) or cysteinylglycine (0.11−0.42 mM) using a stopped flow accessory. The absorbance at 412 nm was recorded for 5−15 min at 25 °C and fitted to a single-exponential plus straight line equation. This approach was also used to evaluate whether HSA−SOH reacted with alanine (10 mM), histidine (20 mM), lysine (10 mM), or arginine (10 mM).

Electrospray Ionization Mass Spectrometry (ESI-MS) Analysis. For the analysis of the intact protein in samples exposed to TNB, oxidized or reduced HSA (50 μM) was incubated with TNB (70 μM) at 25 °C. Aliquots were removed at 10 min and 2 h, treated or not treated with dithiothreitol (DTT, 10 mM, 20 min), and passed twice through Micro Bio-Spin columns equilibrated with 1% acetic acid. Samples were diluted in 1% acetic acid and 50% methanol to a final concentration of 1 μM and introduced using a syringe pump at a flow rate of 10 μL min^{-1} into a QTRAP 2000 mass spectrometer (Applied Biosystems/MDS Sciex). Positive ion ESI mass spectra were collected using an *m*/*z* range of 1000−1700, with ion spray voltage (IS) 5500 V, declustering potential (DP) 50 V, and entrance potential (EP) 10 V. Data acquisition was set to 2 min with a 140 mass spectrum average, and the final mass of intact HSA was calculated by automatic deconvolution using Analyst 1.4 software.

For the analysis of the tryptic fragment containing Cys34 in HSA samples exposed to hydrogen peroxide for increasing times, the protein was diluted to 75 μM in ammonium bicarbonate (50 mM, pH 8.2) and incubated overnight with trypsin (HSA to trypsin ratio of 200:1). The peptide mixture was diluted 26-fold in 1% acetic acid and 50% methanol, injected into the mass spectrometer, and analyzed directly in the enhanced resolution (ER) mode to obtain high-resolution mass spectra and confirm the peptide charges. MS/MS for a specific ion was obtained in the enhanced product ion (EPI) mode using an *m*/*z* range of 100−1700, with IS = 5000 V, DP = 20 V, temperature 150 °C, and collision energy (CE) 50 V.

Matrix-Assisted Laser Desorption Ionization Time of Flight Mass Spectrometry (MALDI-TOF-MS) Analysis. Mass spectra of digestion mixtures were acquired on a 4800 MALDI-TOF−TOF analyzer system (Applied Biosystems) using a matrix solution of α-cyano-4-hydroxycynnamic acid in 50% acetonitrile and 0.2% trifluoroacetic acid.

Data Processing. Data were plotted and analyzed using OriginPro 6.1 (Microcal Software). Results are expressed as the average ± standard deviation of independent experiments.

RESULTS

NBD−Cl Is Not Suitable as a Chromophoric Probe for HSA−SOH. To find a technique to quantify HSA−SOH, we first attempted to trap HSA−SOH with NBD−Cl. The sulfoxide product formed between sulfenic acid and NBD−Cl absorbs at ∼350 nm (*18*, *19*, *21*), while the product with the thiol, a thioether, absorbs at greater wavelengths. For reduced HSA, we observed a maximum at 400 nm, probably involving the product between HSA−SH and NBD−Cl (Figure 1A). As expected, treatment of HSA with hydrogen peroxide led to a shift in absorbance to 353 nm suggestive of HSA−SOH formation. Nevertheless, $HgCl_2$- and NEM-blocked HSA yielded similar results, showing that the absorbance increase at ∼350 nm was not due to the formation of HSA−SOH. Rather, it was due to tight noncovalent binding of NBD−Cl, which absorbs at 343 nm in aqueous solution, since the peak disappeared when the samples were denatured with sodium dodecyl sulfate (1%, 20 min, 37 °C)

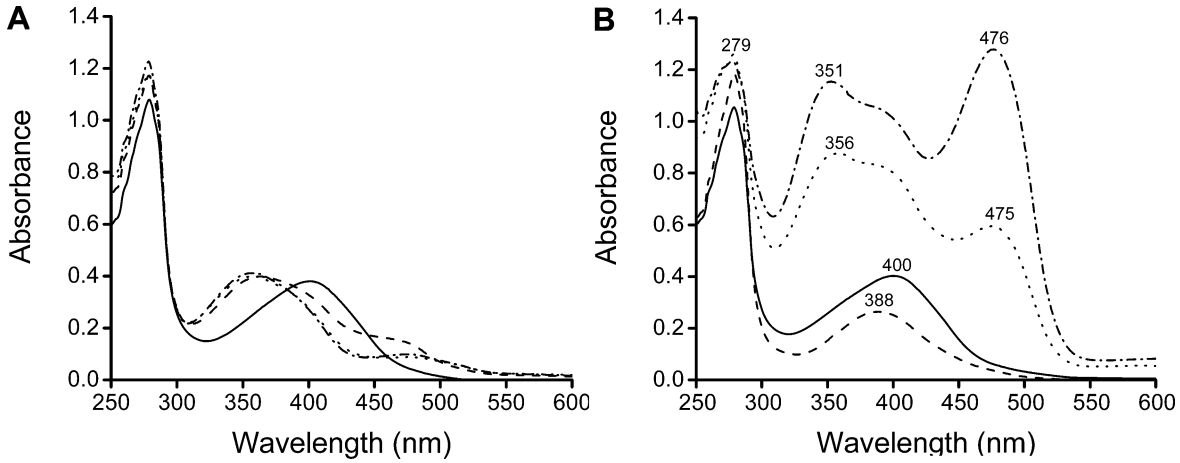

FIGURE 1: UV−vis spectra of the products formed from HSA and NBD−Cl. (A) NBD−Cl (1 mM) was incubated (30 min, 37 °C) with reduced HSA (0.5 mM, 0.8 HSA−SH/HSA, —), $HgCl_2$-blocked HSA (···), oxidized HSA (4 mM H_2O_2, 4 min, 37 °C, ---), and $HgCl_2$-blocked and oxidized HSA (—·—), followed by gel filtration to remove unreacted NBD−Cl. (B) HSA (0.5 mM, 0.86 HSA−SH/HSA) was incubated with 0.5 (---), 1 (—), 4 (···) or 10 (—·—) mM NBD−Cl for 30 min at 37 °C and then subjected to gel filtration.

and washed by ultrafiltration (not shown). Accordingly, when reduced HSA was exposed to greater than stoichiometric NBD−Cl concentrations, the absorbance at ∼350 nm increased (Figure 1B). In addition, new products were observed at 480 nm, probably with amino groups (*41*−*43*). Instead, at stoichiometric NBD−Cl concentrations, a peak was recorded at 388 nm, suggesting that NBD−Cl reacted preferentially with a tyrosine (*42*). This was confirmed by ∼80% inhibition of the esterase-like activity of HSA (not shown), which depends on the very reactive tyrosine 411 (*39*, *40*). As for the peak at 400 nm, since the reported absorbance for the product with thiols is 420 nm (*22*, *43*, *44*), it is possible that it corresponds to the sum of the product with the thiol and the product with tyrosine. Taken together, our results show a variety of nonspecific reactions and that NBD−Cl is not a suitable chromophore for HSA−SOH.

Characterization of the Reaction between HSA−SOH and TNB. A strategy for HSA−SOH quantification was developed on the basis of its reaction with TNB. Sulfenic acid reacts with TNB as an electrophile. This is of relevance because of limited electrophilic groups in proteins. Furthermore, thiols do not react with other thiols, so reduced thiols do not interfere. When oxidized HSA (50 μM) was mixed with TNB (70 μM), absorbance at 412 nm decreased (Figure 2). Plots of TNB concentration versus time were biphasic, with a relatively fast phase that lasted ∼15 min followed by a 20-fold slower phase still occurring after 2 h. The kinetic trace fitted a biexponential equation (eq 1) in agreement with

$$[\mathrm{TNB}] = A_1 \exp(-k_{\mathrm{obs1}}t) + A_2 \exp(-k_{\mathrm{obs2}}t) + \mathrm{offset} \quad (1)$$

two consecutive or parallel reactions, where A_1 and A_2 are the amplitudes and k_{obs1} and k_{obs2} are the pseudo-first-order rate constants of the first and second phases, respectively. In addition, when the first 15 min of data were fitted to a single-exponential plus straight line equation (eq 2), where

$$[\mathrm{TNB}] = A_1 \exp(-k_{\mathrm{obs1}}t) + St + \mathrm{offset} \quad (2)$$

S represents the slope of the linear term, the kinetic parameters obtained for the first phase (amplitude and exponential rate constant) did not change (Figure 2, inset).

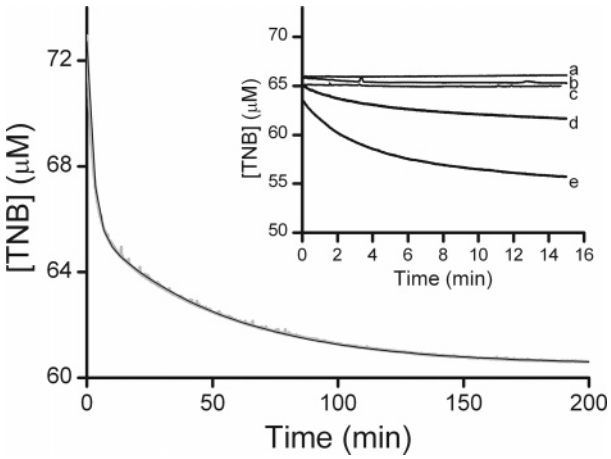

FIGURE 2: Reaction of oxidized HSA with TNB. HSA (0.5 mM, 0.65 HSA−SH/HSA) was oxidized with hydrogen peroxide (4 mM, 4 min, 37 °C), and the reactions were stopped with catalase. Aliquots (50 μM) were incubated with TNB (73 μM), and the decrease in TNB concentration was recorded at 412 nm, 25 °C, and pH 7.4 (gray trace). The black trace represents the best fit to the biexponential (eq 1) function [TNB] = 7.0 exp(−0.40*t*) + 5.3 exp(−0.019*t*) + 60. (Inset) Controls with 65 μM TNB and 50 μM: (a) reduced HSA; (b) NEM-blocked HSA; (c) NEM-blocked and oxidized HSA (4 mM H_2O_2, 4 min, 37 °C); (d) overoxidized HSA (15 mM H_2O_2, 4 min, 37 °C); (e) oxidized HSA (4 mM H_2O_2, 4 min, 37 °C).

Although TNB was the reagent whose consumption was being recorded, it was also the reagent in excess (pseudo-first-order conditions). Therefore, by dividing the exponential rate constants by the TNB concentration when half the reaction had occurred, it was possible to determine the second-order rate constants for the first and second phases, 105 ± 11 M^{-1} s^{-1} (n = 18) and 4.3 ± 0.9 M^{-1} s^{-1} (n = 4), respectively.

Controls using reduced or NEM-blocked HSA, with or without exposure to hydrogen peroxide, did not lead to significant decreases in absorbance at 412 nm, showing that TNB did not react with internal disulfides nor with other oxidized amino acids (Figure 2, inset). Thus, the first phase was assigned to the reaction of interest between HSA−SOH and TNB to form a mixed disulfide (Scheme 1).

From the amplitude of the first phase, the ratio HSA−SOH/HSA was determined as 0.18 ± 0.02 (n = 25). This

Scheme 1: Reaction between HSA−SOH and TNB

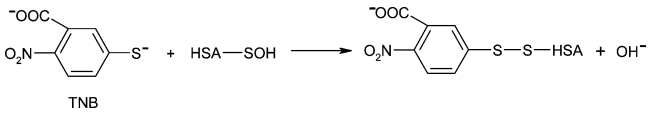

represented 32% of the oxidized thiols, since after exposure to hydrogen peroxide (4 mM, 4 min, 37 °C) the amount of thiols per HSA decreased from 0.66 ± 0.09 to 0.09 ± 0.02 HSA−SH/HSA (n = 4). When reduced HSA was oxidized with 15 mM instead of 4 mM hydrogen peroxide, the amplitude decreased, leading to 0.05 HSA−SOH/HSA. Therefore, at increased hydrogen peroxide concentrations, the thiol was partially oxidized to higher oxidation states such as HSA−SO_2H and HSA−SO_3H, which did not react with TNB. Last, oxidation of 0.5 mM HSA with another oxidant such as peroxynitrite ($ONOO^-$, 1 mM) led to the detection of 0.14 HSA−SOH/HSA (not shown).

When the reaction was performed at increasing TNB concentrations, a proportional increase in the pseudo-first-order rate constant was observed (Figure 3A), while the amplitude did not change (Figure 3A, inset), confirming that the reaction is first-order in TNB. From the slope of the k_{obs} versus TNB concentration plot, the second-order rate constant for the reaction of HSA−SOH with TNB was determined as 104 M^{-1} s^{-1} (25 °C, pH 7.4), confirming the value reported above. The fact that the intercept was close to zero suggested that the reaction was, within experimental error, irreversible. In contrast, when the concentration of oxidized HSA was varied, the amplitude increased linearly (Figure 3B), corroborating that the amplitude of the first phase is stoichiometric with HSA−SOH/HSA was confirmed to be 0.18. From the slope, the amount of HSA−SOH formed per HSA was confirmed to be 0.18. As expected for a reaction first order in HSA−SOH, the pseudo-first-order rate constant did not change with concentration (Figure 3B, inset). In addition to determining the HSA−SOH concentration from the amplitude of the first phase, it can also be calculated from the initial rate of TNB consumption, when less than 10% of the product has been consumed, after division by the TNB concentration and by the second-order rate constant (*45*) (Figure 3C). In fact, using this approach, we determined that 0.18 HSA−SOH/HSA was formed, in excellent agreement with the values obtained from the other plots.

At higher temperatures and TNB concentrations, a greater consumption of TNB was observed in parallel with an increase in the absorbance at 279 nm (not shown), suggesting that the protein was partially denatured and exposed internal disulfide bonds that reacted with TNB. For this reason, reactions were always performed at 25 °C and ∼70 μM TNB.

To confirm the formation of the mixed disulfide between TNB and HSA−SOH in the first phase of the reaction, we performed mass spectrometric analysis of the intact protein. Aliquots of oxidized HSA treated with TNB for 10 min exhibited a peak with a mass increase of 194 ± 4 Da corresponding to ∼46% of the total protein. This peak, consistent with the addition of one TNB (198 Da), was partially reversed with DTT, confirming the formation of a mixed disulfide. However, this peak was also observed, although to lower extents (∼25% of the total protein), when reduced HSA was treated with TNB, suggesting that TNB binds tightly to HSA, even in the acidic analytical conditions.

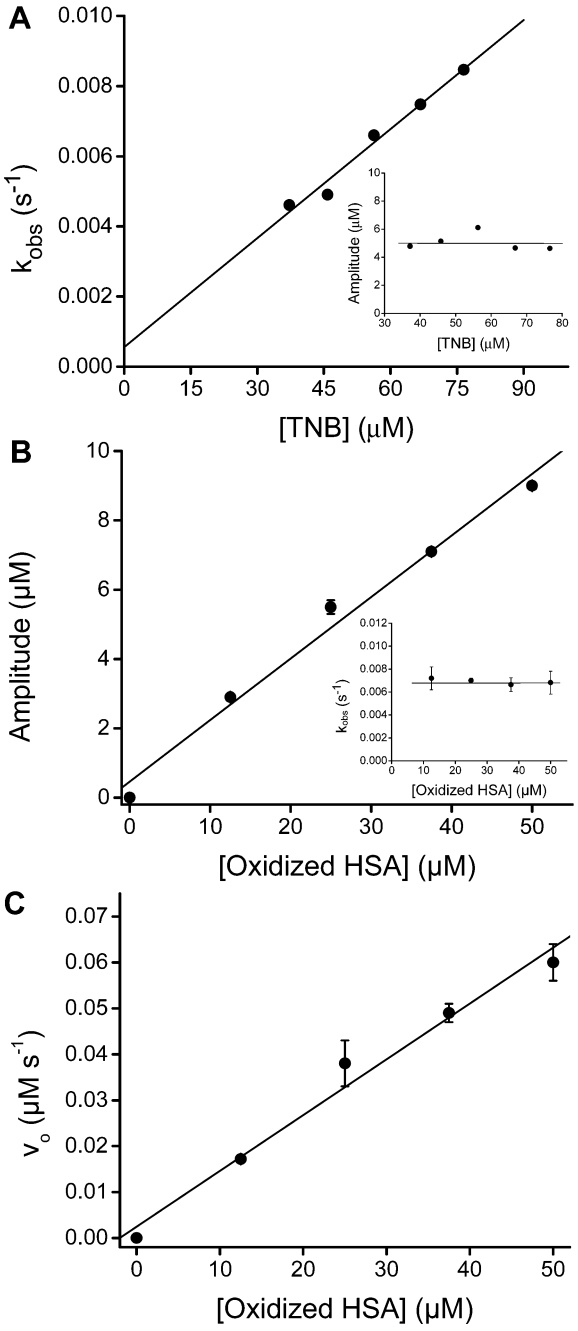

FIGURE 3: Dependence of the reaction between TNB and oxidized HSA on the concentrations. (A) Aliquots (37.5 μM) of oxidized HSA (4 mM H_2O_2, 4 min, 37 °C) were added to increasing concentrations of TNB, and the absorbance was recorded for 15−30 min (412 nm, 25 °C, pH 7.4). The k_{obs} and amplitude (inset) of the first phase of the reaction for each TNB concentration were obtained from the fit to an exponential plus straight line function (eq 2). (B) Aliquots of increasing concentrations of oxidized HSA were added to TNB (70 μM). The absorbance at 412 nm was recorded, and the amplitude and k_{obs} (inset) of the reaction were determined. (C) The first 30 s of the data in (B) were fitted to a straight line to determine the initial rate (v_o).

As for the second phase, we evaluated whether it was due to the reaction between the mixed HSA−TNB disulfide and a second TNB to form DTNB and reduced HSA. However, at long reaction times (2 h), we did not recover reduced HSA according to mass spectrometric measurements confirmed spectrophotometrically (not shown). Thus, the nature of the second phase of the reaction between HSA−SOH and TNB

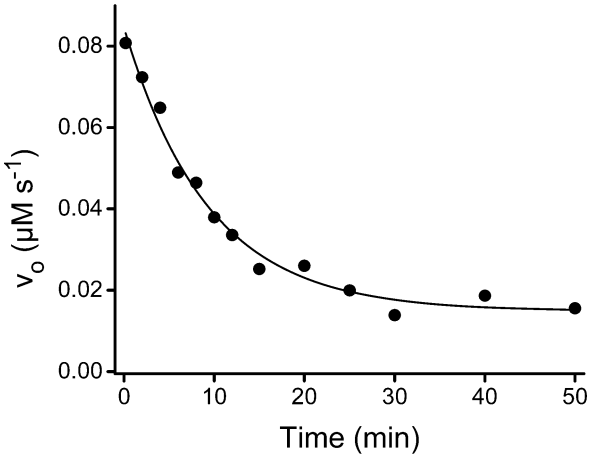

FIGURE 4: Stability of HSA−SOH at 37 °C. Oxidized HSA was incubated at 37 °C. At increasing times, aliquots (50 μM) were mixed with TNB (70 μM) and the initial rate of the absorbance decay at 412 nm and 25 °C was measured. The solid line represents the best fit to the single-exponential function $v_0 = 0.070 \exp(-0.11t) + 0.015$.

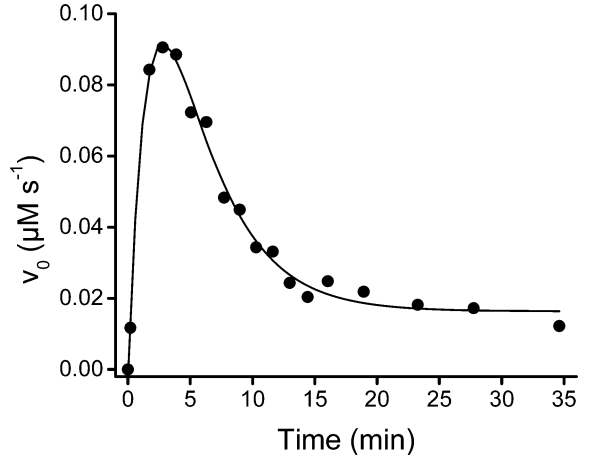

FIGURE 5: Reaction of HSA−SH and HSA−SOH with hydrogen peroxide. HSA (0.5 mM, 0.77 HSA−SH/HSA) was incubated with hydrogen peroxide (4 mM) at 37 °C. At increasing times, aliquots (50 μM HSA) were mixed with catalase and TNB (70 μM) and the initial rate of the absorbance decay at 412 nm and 25 °C was measured. The solid line represents the best fit to the biexponential function $v_0 = -0.30 \exp(-0.56t) + 0.28 \exp(-0.25t) + 0.016$.

is not well defined, but does not prevent the use of TNB as a sulfenic acid probe. Last, we determined the rate constant of the reaction between DTNB and HSA−SH as 14.8 ± 0.8 M^{-1} s^{-1} at 25 °C, pH 7.4, and ionic strength ~0.25 (not shown).

Stability of HSA−SOH. Using the reaction with TNB, we studied the stability of HSA−SOH. Oxidized HSA was incubated at 4, 25, or 37 °C, and the initial rate of TNB consumption, indicative of the HSA−SOH concentration, was followed. HSA−SOH was stable in phosphate buffer at 4 °C, with more than 95% remaining after 1 h, but gradually disappeared at 25 and 37 °C. Further analysis showed that at 37 °C the first-order rate constant of spontaneous decay was (1.7 ± 0.3) × 10^{-3} s^{-1} (n = 10, Figure 4). Similar results were obtained when unreacted hydrogen peroxide was eliminated by gel filtration rather than by addition of catalase. It is noteworthy that, even at long reaction times, when most HSA−SOH had decayed, we systematically observed that the solutions maintained a certain ability to consume TNB (~0.016 μM s^{-1}). The reason for this consumption is unknown. Preliminary experiments suggest that it could be related to the second phase of the reaction between TNB and oxidized HSA. Samples allowed to decay at 37°C for 40 min were analyzed through SDS−PAGE and ESI and MALDI-TOF MS. No dimers were observed through SDS−PAGE under reducing or nonreducing conditions, and no peptides with the masses expected for possible sulfenic acid derivatives (−2, +14, +30, +32, or +48 Da; see the discussion below) of the Cys34 tryptic fragment could be detected through MS.

Reaction of HSA−SOH with hydrogen peroxide. Previous work has shown that HSA−SH reacts with hydrogen peroxide, yielding HSA−SOH with a second-order rate constant of 2.26 M^{-1} s^{-1} (37 °C, pH 7.4) (*22*):

$$\text{HSA}-\text{SH} + \text{H}_2\text{O}_2 \rightarrow \text{HSA}-\text{SOH} + \text{H}_2\text{O} \qquad (3)$$

In addition, HSA−SOH can react with a second hydrogen peroxide, yielding sulfinic acid (HSA−SO_2H):

$$\text{HSA}-\text{SOH} + \text{H}_2\text{O}_2 \rightarrow \text{HSA}-\text{SO}_2\text{H} + \text{H}_2\text{O} \qquad (4)$$

To determine the rate constants for these two reactions, we followed the initial rate of TNB consumption, indicative of the HSA−SOH concentration. As shown in Figure 5, when reduced HSA was mixed with hydrogen peroxide, the initial rate first increased with time as expected but then decreased due to further oxidation of HSA−SOH with excess hydrogen peroxide. The plot of the initial rate versus time fitted a biexponential function (eq 1) with amplitudes of opposite sign, in agreement with the two consecutive reaction mechanism with HSA−SOH as the intermediate (eqs 3 and 4) (*45*). From the nonlinear least-squares analysis, and after correction for the spontaneous decay of HSA−SOH, the rate constants for both processes were determined. Thus, the formation of HSA−SOH occurred with a second-order rate constant of 2.7 ± 0.7 M^{-1} s^{-1} (n = 4, 37 °C, pH 7.4), in accordance with the previous report (*22*). In turn, the reaction of HSA−SOH with hydrogen peroxide occurred with a second-order rate constant of 0.4 ± 0.2 M^{-1} s^{-1} (n = 4, 37 °C, pH 7.4). The maximum yield of HSA−SOH/HSA expected for these two consecutive reactions was calculated as 0.42 ± 0.08 (*45*). However, the maximum yield obtained experimentally was 0.20 ± 0.04 HSA−SOH/HSA. Experiments with higher hydrogen peroxide concentrations had interference by evolution of dioxygen after the reaction of catalase with hydrogen peroxide.

Mass spectrometry analysis confirmed the formation of HSA−SO_2H (eq 4). In tryptic digests of HSA exposed to 4 mM hydrogen peroxide for 30 min, a peptide with the mass expected for the Cys34-containing fragment (residues 21−41, ALVLIAFAQYLQQC$_{34}$PFEDHVK, 2432.3 Da) + 32 Da was detected through ESI-MS as the doubly charged $[M + 2H]^{2+}$ species, m/z 1233.2 (Figure 6). The peptide could be detected, although with ~3-fold lower intensity, in control and 4 min samples, in accordance with HSA−SO_2H being present in stock solutions. MS/MS of the $[M + 2H]^{2+}$ parent ion led to the detection of several b and y daughter ions that confirmed the identity of the fragment (Figure 6B). The b_{14} ion (1594.4) clearly showed the +32 Da mass increase associated with the Cys34 sulfinic acid modification. It is noteworthy that the fragmentation pattern showed one major

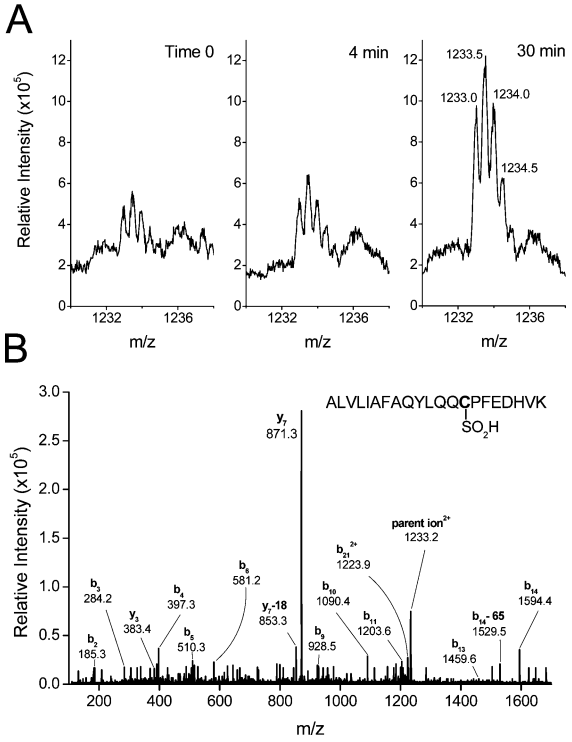

FIGURE 6: Mass spectrometric analysis of HSA−SO_2H. (A) HSA was incubated with hydrogen peroxide as in Figure 5. Aliquots were removed at 0 (left), 4 (center) and 30 (right) min, digested with trypsin, and analyzed by ESI-MS. The Cys34-containing peptide with a mass increase of +32 Da was detected as the doubly charged species (*m*/*z* 1233.2). (B) MS/MS spectrum of the doubly charged parent ion at *m*/*z* 1233.2 showing the b and y fragments.

Table 1: Reactivity of HSA−SOH at pH 7.4

target molecule	rate constant (M^{-1} s^{-1})	target molecule	rate constant (M^{-1} s^{-1})
thionitrobenzoate	105 ± 11^a	glutathione	2.9 ± 0.5^a
dimedone	0.027 ± 0.009^b	homocysteine	9.3 ± 0.9^a
sodium arsenite	0.036 ± 0.009^b	cysteinylglycine	55 ± 3^a
ascorbate	ND[c]	alanine	ND[c]
urate	ND[c]	histidine	ND[c]
hydrogen peroxide	0.4 ± 0.2^b	lysine	ND[c]
cysteine	21.6 ± 0.2^a	arginine	ND[c]

[a] Rate constant determined at 25 °C. [b] Rate constant determined at 37 °C. [c] Not detected.

species, the y_7 ion. This, together with the b_{14} ion, suggests that the peptide was predominantly fragmented at the cysteinesulfinic acid−proline bond. In addition, an ion with a mass corresponding to b_{14} − 65 Da was observed, consistent with loss of the SO_2H moiety. Through MALDI-TOF-MS (not shown), the tryptic fragment containing cysteinesulfinic acid was only detected in the sample exposed to hydrogen peroxide for 30 min, but not in the control nor 4 min sample. The MS/MS analysis led to the detection of only two ions, the y_7 and b_{14} ions, confirming the results obtained by ESI-MS.

Reaction of HSA−SOH with Dimedone and Sodium Arsenite. The reactions with dimedone and arsenite, two reagents typically used for sulfenic acid detection, were relatively slow, although appreciable rate constants were measured for both (Table 1). Controls showed that neither dimedone nor arsenite reacted with TNB nor DTNB. In the case of dimedone, no effect of the ethanol solvent was

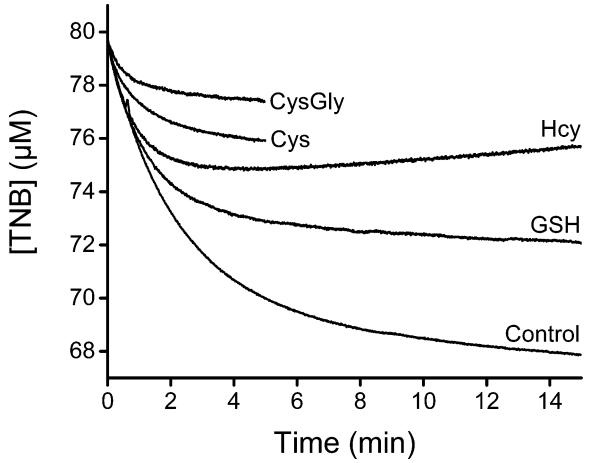

FIGURE 7: Competition between TNB and biologically relevant thiols for reaction with HSA−SOH. Aliquots of oxidized HSA (50 μM) were mixed with TNB (70 μM) at 25 °C in the absence or presence of cysteine (1 mM), glutathione (1 mM), homocysteine (1 mM), or cysteinylglycine (0.42 mM) using a stopped flow accessory. The decay in absorbance at 412 nm was followed for 5−15 min.

detected, and in the case of arsenite, the pH was controlled to prevent alkalinization. Arsenite partially reduced HSA−SOH back to thiol, since incubation of oxidized HSA with 0.167 M arsenite (10 min, 37 °C) led to an increase in HSA−SH/HSA of 0.051. This represents a 28% recovery with respect to the initial amount of HSA−SOH/HSA (0.18 ± 0.02), which can be explained in part because the spontaneous decay of HSA−SOH ($k = 1.7 \times 10^{-3}$ s^{-1}) competed with the reaction with arsenite ($k = 0.036$ M^{-1} s^{-1}).

Reaction of HSA−SOH with Urate and Ascorbate. Millimolar concentrations of the plasma reductants ascorbate and urate did not increase the rate of HSA−SOH decay at 37 °C and pH 7.4. Furthermore, they did not reduce HSA−SOH back to HSA−SH as measured with DTNB (not shown). The pH was controlled in these experiments, and no reaction was observed between the reductants and TNB or DTNB.

Reaction of HSA−SOH with Thiols. The plasma thiols cysteine, glutathione, homocysteine, and cysteinylglycine competed with TNB for the reaction with HSA−SOH (Figure 7). Despite the fact that only TNB consumption was followed, the observed rate constant of the first phase was the sum of the pseudo first-order rate constants of HSA−SOH reaction with TNB and thiol, so that k_{obs} increased linearly with the thiol concentration. From the slope, we determined that the second-order rate constant for the reaction of cysteine and HSA−SOH was 21.6 ± 0.2 M^{-1} s^{-1} at 25 °C and pH 7.4 (Figure 8, Table 1). The amplitude of the first phase decreased hyperbolically in the presence of cysteine (Figure 8, inset), as expected for the competition mechanism (*45*), giving a value for the second-order rate constant of 22 ± 6 M^{-1} s^{-1}, in agreement with the value obtained from k_{obs}. Similar profiles were obtained for glutathione, homocysteine, and cysteinylglycine, giving rate constants of 2.9 ± 0.5, 9.3 ± 0.9, and 55 ± 3 M^{-1} s^{-1} (25 °C, pH 7.4), respectively (Table 1). It is worth noting that the second phase of the reaction presented a positive slope in the case of homocysteine (Figure 7), probably reflecting the tendency of this thiol to displace other more acidic thiols from mixed disulfides. As control, there was

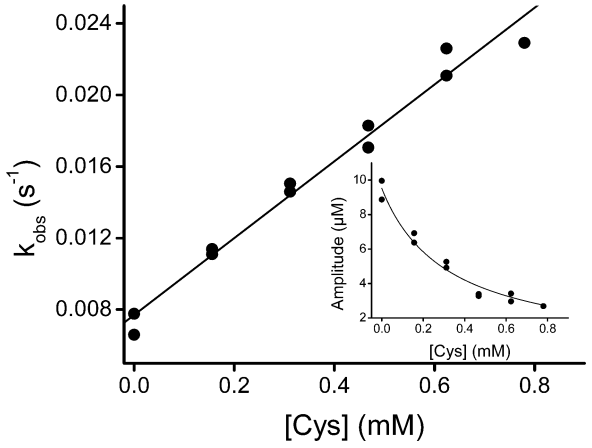

FIGURE 8: Reaction of HSA−SOH with cysteine. Aliquots of oxidized HSA (50 μM) were mixed with TNB (70 μM) at 25 °C in the presence of increasing concentrations of cysteine using a stopped flow accessory. The decay in absorbance at 412 nm was followed for 5−15 min, and the observed rate constant (k_{obs}) and amplitude (inset) were determined from the fit to an exponential plus straight line function (eq 2).

no detectable reaction between TNB and the cysteine, glutathione, homocysteine, and cysteinylglycine solutions.

Reaction of HSA−SOH with Amines. No increases were detected in the observed rate constant of TNB consumption in the presence of high millimolar concentrations of alanine, histidine, lysine, and arginine. This confirms that the reactions of HSA−SOH with the thiol-containing amino acids and peptides were due to the thiol moieties.

DISCUSSION

Spectrophotometric detection of HSA−SOH with NBD−Cl is shown herein to lack specificity so that mass spectrometry is needed for the unequivocal detection of the sulfoxide product (*46*). Although our results may not be generalized to all proteins, they are of relevance because NBD−Cl is widely used as a sulfenic acid probe.

The reaction with TNB ($k = 105 \pm 11$ M^{-1} s^{-1}, 25 °C, pH 7.4) was specific for HSA−SOH, since TNB did not react with reduced, thiol-blocked, or overoxidized HSA. TNB has been previously used to detect and quantify sulfenic acid in other proteins using end point measurements (*14*−*17*). However, the reaction of TNB with HSA−SOH required several minutes and was biphasic, revealing the importance of kinetic analysis. Thus, before using TNB for sulfenic acid measurement, it is imperative to understand reaction kinetics for specific proteins. In addition, TNB should be used with caution with complex mixtures and cell extracts, where other electrophiles and disulfides are likely to interfere.

TNB permitted, for the first time, quantitative insight regarding the amount of sulfenic acid formed by oxidation of HSA. With 4 mM hydrogen peroxide (4 min, 37 °C), the yield of HSA−SOH/HSA was 0.18 ± 0.02. This yield can be accounted for by several factors including the rate of HSA−SOH formation, its spontaneous decay, and its reaction with a second hydrogen peroxide, leading to HSA−SO_2H.

Although relatively stable, HSA−SOH decayed in phosphate buffer with a first-order rate constant of $(1.7 \pm 0.3) \times 10^{-3}$ s^{-1} at 37 °C. Electrophoretic analysis ruled out further reaction of HSA−SOH with a second molecule of HSA−SH or HSA−SOH to form intermolecular disulfide or thiosulfinate dimers, probably because of steric hindrance. A possible explanation for this slow decay of HSA−SOH could be the condensation with an amine or amide nitrogen (*11*). Although no reaction was detected with the free amino acids alanine, histidine, lysine, and arginine, it is still possible that HSA−SOH could react slowly with an internal residue. The formation of a cyclic sulfenamide on a sulfenic acid after the reaction with the neighboring amide nitrogen has been recently reported (*47*, *48*), although this can be ruled out in the case of HSA because the neighboring residue is a proline. No Cys34 tryptic fragments with mass changes of −2, +14, or +30 Da were detected, suggesting that sulfenamide or its oxidized derivatives are not formed within the same peptide.

In addition, HSA−SOH can react with a second hydrogen peroxide to yield HSA−SO_2H with a second-order rate constant of 0.4 ± 0.2 M^{-1} s^{-1} (37 °C, pH 7.4). This rate constant is ∼7-fold lower than that between HSA−SH and hydrogen peroxide (2.7 ± 0.7 M^{-1} s^{-1}, 37 °C, pH 7.4), in agreement with the expected decreased nucleophilicity of the oxyacid compared to the thiol. This reaction may contribute to the formation of the higher oxidation states of HSA that have been observed in vivo. It is noteworthy that the formation of sulfinic acid is involved in the inactivation of peroxiredoxins.

From the initial rate of TNB consumption, the maximum yield of HSA−SOH formed after incubation with hydrogen peroxide was estimated. When both the spontaneous decay of HSA−SOH and its reaction with hydrogen peroxide were taken into account, there was a maximum yield of 0.20 ± 0.04 HSA−SOH/HSA, ∼50% of that expected. One explanation for this discrepancy could be that different HSA−SH populations exist with respect to oxidant reactivity. In this sense, ^{1}H NMR shows that the HSA thiol is in equilibrium between buried and exposed forms (*49*, *50*). Undoubtedly, the properties of the thiol and its derivatives in a protein such as HSA are complex.

The reaction with TNB permitted determination of the second-order rate constants for the reaction of HSA−SOH with sodium arsenite and dimedone (0.036 ± 0.009 and 0.027 ± 0.009 M^{-1} s^{-1}, respectively) at 37 °C and pH 7.4. This reaffirms that these reagents are useful sulfenic acid probes. In contrast, ascorbate and urate did not react with HSA−SOH at appreciable rates. Considering plasma concentrations (ascorbate, 30−150 μM; urate, 160−450 μM (*51*)), it can be concluded that these reductants will not significantly react with HSA−SOH in vivo. Nevertheless, ascorbic acid has been recently reported to sustain peroxiredoxin activity (*52*). As for the free amino acids alanine, histidine, lysine, and arginine, it can also be concluded that they will not react with HSA−SOH at their plasma concentrations of 316, 87, 195, and 86 μM, respectively (*53*).

HSA−SOH reacts with glutathione, leading to a mixed disulfide (*22*). Herein, the rate constants for HSA−SOH reaction with cysteine, glutathione, homocysteine, and cysteinylglycine were determined as 21.6 ± 0.2, 2.9 ± 0.5, 9.3 ± 0.9, and 55 ± 3 M^{-1} s^{-1}, respectively (25 °C and pH 7.4). It is interesting to compare these values with that reported for the reaction of cysteinesulfenic acid with cysteine, ≥720 M^{-1} s^{-1} (*54*, *55*). Likely, the more sterically hindered environment of the protein will diminish the reactivity of sulfenic acid toward thiols. Considering the

corresponding macroscopic pK_a of the thiols (*9*, *56*), cysteinylglycine (pK_a = 7.1−7.9 (*57*, *58*)) reacted faster than cysteine (pK_a = 8.1−8.4 (*2*, *57*, *59*, *60*)), glutathione (pK_a = 8.6−9.2 (*57*, *59*−*61*)), and homocysteine (pK_a = 8.7−10.0 (*57*, *59*)), in agreement with the anionic thiolate being the reactive species toward HSA−SOH. Indeed, TNB (pK_a 4.5−5.1 (*62*, *63*)) reacted even faster (105 ± 11 M^{-1} s^{-1}). Glutathione was the slowest, probably due to steric restrictions and the additional anionic charge of glutathione at pH 7.4.

The rate constants summarized in Table 1 are useful for evaluating the possible fates of HSA−SOH in vivo. Since HSA−SOH will not be reduced back to thiol by ascorbate or urate, or react with free amines, the fate of HSA−SOH will likely be reaction with other thiols. For example, at plasma concentrations of reduced cysteine, glutathione, homocysteine, and cysteinylglycine of 8.2, 4.7, 0.2, and 2.9 μM, respectively (*64*, *65*), the products of the rate constant times concentration are 177 × 10^{-6}, 14 × 10^{-6}, 2 × 10^{-6}, and 160 × 10^{-6} s^{-1}. This agrees with the observation that mixed disulfides in circulating HSA are predominantly derivatives of cysteine (146 μM) and cysteinylglycine (19.7 μM) rather than glutathione (0.7 μM) and homocysteine (7.4 μM) (*64*, *65*). Thiol/disulfide exchange reactions also contribute to the formation of mixed HSA disulfides, as can be seen from the fact that disulfides with homocysteine are at such a high relative concentration, reflecting the tendency of homocysteine to form disulfides due to its higher pK_a (*2*, *58*, *66*).

In conclusion, we determined that NBD−Cl is not a suitable reagent for sulfenic acid detection in HSA. In turn, we developed a strategy using TNB that allowed HSA−SOH to be quantified and hence its reactivity and kinetics with several molecules of analytical or biological interest to be studied. In addition, the formation of products such as mixed disulfides and sulfinic acid was characterized. Since knowledge of the biological reactivity of sulfenic acid is limited, this systematic study aids in the design of approaches for sulfenic acid detection besides illustrating the possible biological fates of this key redox intermediate.

ACKNOWLEDGMENT

We thank Dr. Madia Trujillo for helpful discussions.

REFERENCES

1. Surdhar, P., and Armstrong, D. (1986) Redox potentials of some sulfur-containing radicals, *J. Phys. Chem. 90*, 5915−5917.
2. Keire, D., Strauss, E., Guo, W., Noszal, B., and Rabenstein, D. (1992) Kinetics and equilibria of thiol/disulfide interchange reactions of selected biological thiols and related molecules with oxidized glutathione, *J. Org. Chem. 95*, 123−127.
3. Paget, M. S., and Buttner, M. J. (2003) Thiol-based regulatory switches, *Annu. Rev. Genet. 37*, 91−121.
4. Ghezzi, P., Bonetto, V., and Fratelli, M. (2005) Thiol-disulfide balance: from the concept of oxidative stress to that of redox regulation, *Antioxid. Redox Signaling 7*, 964−972.
5. Claiborne, A., Miller, H., Parsonage, D., and Ross, R. P. (1993) Protein-sulfenic acid stabilization and function in enzyme catalysis and gene regulation, *FASEB J. 7*, 1483−1490.
6. Claiborne, A., Yeh, J. I., Mallett, T. C., Luba, J., Crane, E. J., 3rd, Charrier, V., and Parsonage, D. (1999) Protein-sulfenic acids: diverse roles for an unlikely player in enzyme catalysis and redox regulation, *Biochemistry 38*, 15407−15416.
7. Poole, L. B., Karplus, P. A., and Claiborne, A. (2004) Protein sulfenic acids in redox signaling, *Annu. Rev. Pharmacol. Toxicol. 44*, 325−347.
8. Kice, J., and Cleveland, J. (1973) Nucleophilic substitution reactions involving sulfenic acids and sulfenyl derivatives. Nucleophile- and acid-catalyzed oxygen-18 exchange of phenyl benzenethiolsulfinate, *J. Am. Chem. Soc. 95*, 104−109.
9. Torchinsky, Y. (1981) *Sulfur in Proteins*, Pergamon Press, Ltd., Oxford, U.K.
10. Claiborne, A., Mallett, T. C., Yeh, J. I., Luba, J., and Parsonage, D. (2001) Structural, redox, and mechanistic parameters for cysteine-sulfenic acid function in catalysis and regulation, *Adv. Protein Chem. 58*, 215−276.
11. Allison, W. (1976) Formation and reactions of sulfenic acids in proteins, *Acc. Chem. Res. 9*, 293−299.
12. Poole, L. B., Zeng, B. B., Knaggs, S. A., Yakubu, M., and King, S. B. (2005) Synthesis of chemical probes to map sulfenic acid modifications on proteins, *Bioconjugate Chem. 16*, 1624−1628.
13. Charles, R. L., Schroder, E., May, G., Free, P., Gaffney, P. R., Begum, S., Wait, R., Heads, R. J., and Eaton, P. (2007) Protein sulfenation as a redox sensor: Proteomic studies using a novel biotinylated dimedone analogue, *Mol. Cell. Proteomics* (in press).
14. Ellis, H. R., and Poole, L. B. (1997) Roles for the two cysteine residues of AhpC in catalysis of peroxide reduction by alkyl hydroperoxide reductase from Salmonella typhimurium, *Biochemistry 36*, 13349−13356.
15. Boschi-Muller, S., Azza, S., Sanglier-Cianferani, S., Talfournier, F., Van Dorsselear, A., and Branlant, G. (2000) A sulfenic acid enzyme intermediate is involved in the catalytic mechanism of peptide methionine sulfoxide reductase from Escherichia coli, *J. Biol. Chem. 275*, 35908−35913.
16. Peshenko, I. V., and Shichi, H. (2001) Oxidation of active center cysteine of bovine 1-Cys peroxiredoxin to the cysteine sulfenic acid form by peroxide and peroxynitrite, *Free Radical Biol. Med. 31*, 292−303.
17. Poole, L. B., and Ellis, H. R. (2002) Identification of cysteine sulfenic acid in AhpC of alkyl hydroperoxide reductase, *Methods Enzymol. 348*, 122−136.
18. Ellis, H. R., and Poole, L. B. (1997) Novel application of 7-chloro-4-nitrobenzo-2-oxa-1,3-diazole to identify cysteine sulfenic acid in the AhpC component of alkyl hydroperoxide reductase, *Biochemistry 36*, 15013−15018.
19. Denu, J. M., and Tanner, K. G. (1998) Specific and reversible inactivation of protein tyrosine phosphatases by hydrogen peroxide: evidence for a sulfenic acid intermediate and implications for redox regulation, *Biochemistry 37*, 5633−5642.
20. Bryk, R., Griffin, P., and Nathan, C. (2000) Peroxynitrite reductase activity of bacterial peroxiredoxins, *Nature 407*, 211−215.
21. Fuangthong, M., and Helmann, J. D. (2002) The OhrR repressor senses organic hydroperoxides by reversible formation of a cysteine-sulfenic acid derivative, *Proc. Natl. Acad. Sci. U.S.A. 99*, 6690−6695.
22. Carballal, S., Radi, R., Kirk, M. C., Barnes, S., Freeman, B. A., and Alvarez, B. (2003) Sulfenic acid formation in human serum albumin by hydrogen peroxide and peroxynitrite, *Biochemistry 42*, 9906−9914.
23. Saurin, A. T., Neubert, H., Brennan, J. P., and Eaton, P. (2004) Widespread sulfenic acid formation in tissues in response to hydrogen peroxide, *Proc. Natl. Acad. Sci. U.S.A. 101*, 17982−17987.
24. Peters, T. (1996) *All about Albumin. Biochemistry, Genetics and Medical Applications*, Academic Press, New York.
25. Radi, R., Bush, K. M., Cosgrove, T. P., and Freeman, B. A. (1991) Reaction of xanthine oxidase-derived oxidants with lipid and protein of human plasma, *Arch. Biochem. Biophys. 286*, 117−125.
26. Alvarez, B., Ferrer-Sueta, G., Freeman, B. A., and Radi, R. (1999) Kinetics of peroxynitrite reaction with amino acids and human serum albumin, *J. Biol. Chem. 274*, 842−848.
27. Kawai, K., Yoh, M., Hayashi, T., Imai, H., Negawa, T., Tomida, M., Sogami, M., and Era, S. (2001) Effect of diabetic retinopathy on redox state of aqueous humor and serum albumin in patients with senile cataract, *Tokai J. Exp. Clin. Med. 26*, 93−99.
28. Tomida, M., Ishimaru, J., Hayashi, T., Nakamura, K., Murayama, K., and Era, S. (2003) The redox states of serum and synovial fluid of patients with temporomandibular joint disorders, *Jpn. J. Physiol. 53*, 351−355.
29. Mera, K., Anraku, M., Kitamura, K., Nakajou, K., Maruyama, T., and Otagiri, M. (2005) The structure and function of oxidized

albumin in hemodialysis patients: Its role in elevated oxidative stress via neutrophil burst, *Biochem. Biophys. Res. Commun. 334*, 1322−1328.
30. Musante, L., Bruschi, M., Candiano, G., Petretto, A., Dimasi, N., Del Boccio, P., Urbani, A., Rialdi, G., and Ghiggeri, G. M. (2006) Characterization of oxidation end product of plasma albumin 'in vivo', *Biochem. Biophys. Res. Commun. 349*, 668−673.
31. Cha, M. K., and Kim, I. H. (2006) Disulfide between Cys392 and Cys438 of human serum albumin is redox-active, which is responsible for the thioredoxin-supported lipid peroxidase activity, *Arch. Biochem. Biophys. 445*, 19−25.
32. Claiborne, A. (1985) *Handbook of Methods for Oxygen Radical Research*, CRC Press, Inc., Boca Raton, FL.
33. Aebi, H. (1984) Catalase in vitro, *Methods Enzymol. 105*, 121−126.
34. Chen, R. F. (1967) Removal of fatty acids from serum albumin by charcoal treatment, *J. Biol. Chem. 242*, 173−181.
35. Bunk, D. M. (1997) Characterization of the glycation of albumin in freeze-dried and frozen human serum, *Anal. Chem. 69*, 2457−2463.
36. Riener, C. K., Kada, G., and Gruber, H. J. (2002) Quick measurement of protein sulfhydryls with Ellman's reagent and with 4,4′-dithiodipyridine, *Anal. Bioanal. Chem. 373*, 266−276.
37. Boyer, P. D. (1954) Spectrophotometric study of the reaction of protein sulfhydryl groups with organic mercurials, *J. Am. Chem. Soc. 76*, 4331−4337.
38. Romero, N., Radi, R., Linares, E., Augusto, O., Detweiler, C. D., Mason, R. P., and Denicola, A. (2003) Reaction of human hemoglobin with peroxynitrite. Isomerization to nitrate and secondary formation of protein radicals, *J. Biol. Chem. 278*, 44049−44057.
39. Means, G. E., and Bender, M. L. (1975) Acetylation of human serum albumin by p-nitrophenyl acetate, *Biochemistry 14*, 4989−4994.
40. Watanabe, H., Tanase, S., Nakajou, K., Maruyama, T., Kragh-Hansen, U., and Otagiri, M. (2000) Role of arg-410 and tyr-411 in human serum albumin for ligand binding and esterase-like activity, *Biochem. J. 349 Pt 3*, 813−819.
41. Ghosh, P. B., and Whitehouse, M. W. (1968) 7-chloro-4-nitrobenzo-2-oxa-1,3-diazole: a new fluorigenic reagent for amino acids and other amines, *Biochem. J. 108*, 155−156.
42. Aboderin, A. (1976) Reaction of chicken egg white lysozyme with 7-chloro-4-nitrobenz-2-oxa-1,3-diazole, *Biochim. Biophys. Acta 420*, 177−186.
43. Miki, M. (1985) Chemical modification of tropomyosin with NBD-chloride, *J. Biochem. (Tokyo) 97*, 1067−1072.
44. Birkett, D. J. (1970) The reactivity of SH groups with a fluorogenic reagent, *FEBS Lett. 6*, 346−348.
45. Espenson, J. H. (1995) *Chemical Kinetics and Reaction Mechanisms*, 2nd ed., McGraw-Hill, Inc., New York.
46. Kratochwil, N. I. A. I., Patriarca, M., Parkinson, J. A., Gouldsworthy, A. M., Murdoch, P., Sadler, P. J. (1999) Surprising reactions of iodo Pt(IV) and Pt(II) complexes with human serum albumin: detection of Cys34 sulfenic acid, *J. Am. Chem. Soc. 121*, 8193−8203.
47. Salmeen, A., Andersen, J. N., Myers, M. P., Meng, T. C., Hinks, J. A., Tonks, N. K., and Barford, D. (2003) Redox regulation of protein tyrosine phosphatase 1B involves a sulphenyl-amide intermediate, *Nature 423*, 769−773.
48. Lee, J. W., Soonsanga, S., and Helmann, J. D. (2007) A complex thiolate switch regulates the Bacillus subtilis organic peroxide sensor OhrR, *Proc. Natl. Acad. Sci. U.S.A.* (in press).
49. Christodoulou, J., Sadler, P. J., and Tucker, A. (1994) A new structural transition of serum albumin dependent on the state of Cys34. Detection by 1H-NMR spectroscopy, *Eur. J. Biochem. 225*, 363−368.
50. Christodoulou, J., Sadler, P. J., and Tucker, A. (1995) 1H NMR of albumin in human blood plasma: drug binding and redox reactions at Cys34, *FEBS Lett. 376*, 1−5.
51. Motchnik, P. A., Frei, B., and Ames, B. N. (1994) Measurement of antioxidants in human blood plasma, *Methods Enzymol. 234*, 269−279.
52. Monteiro, G., Horta, B., Carvalho, D., Augusto, O., and Netto, L. (2007) Reduction of 1-Cys peroxiredoxins by ascorbate changes the thiol-specific antioxidant paradigm, revealing a function of vitamin C, *Proc. Natl. Acad. Sci. U.S.A. 104*, 4886−4891.
53. Filho, J. C., Bergstrom, J., Stehle, P., and Furst, P. (1997) Simultaneous measurements of free amino acid patterns of plasma, muscle and erythrocytes in healthy human subjects, *Clin. Nutr. 16*, 299−305.
54. Luo, D., Smith, S. W., and Anderson, B. D. (2005) Kinetics and mechanism of the reaction of cysteine and hydrogen peroxide in aqueous solution, *J. Pharm. Sci. 94*, 304−316.
55. Ashby, M. T., and Nagy, P. (2006) On the kinetics and mechanism of the reaction of cysteine and hydrogen peroxide in aqueous solution, *J. Pharm. Sci. 95*, 15−18.
56. Dixon, H. B. (1976) The unreliability of estimates of group dissociation constants, *Biochem. J. 153*, 627−629.
57. Benesch, R. E., and Benesch, R. (1955) The acid strength of the -SH group in cysteine and related compounds, *J. Am. Chem. Soc. 77*, 5877−5881.
58. Sengupta, S., Wehbe, C., Majors, A. K., Ketterer, M. E., DiBello, P. M., and Jacobsen, D. W. (2001) Relative roles of albumin and ceruloplasmin in the formation of homocystine, homocysteine-cysteine-mixed disulfide, and cystine in circulation, *J. Biol. Chem. 276*, 46896−46904.
59. Friedman, M., Cavins, J. F., and Wall, J. S. (1965) Relative nucleophilic reactivities of amino groups and mercaptide ions in addition reactions with α,β-unsaturated compounds, *J. Am. Chem. Soc. 87*, 3672−3682.
60. Jung, G., Breitmaier, E., and Voelter, W. (1972) Dissociation equilibrium of glutathione. A Fourier transform-13C-NMR spectroscopic study of pH-dependence and of charge densities, *Eur. J. Biochem. 24*, 438−445.
61. Rabenstein, D. (1973) Nuclear magnetic resonance studies of the acid-base chemistry of amino acids and peptides. I. Microscopic ionization constants of glutathione and methylmercury-complexed glutathione, *J. Am. Chem. Soc. 95*, 2797−2803.
62. Wilson, J., Wu, D., Motiu-DeGrood, R., and Hupe, D. J. (1980) A spectrophotometric method for studying the rates of reaction disulfides with protein thiol groups applied to bovine serum albumin, *J. Am. Chem. Soc. 102*, 359−363.
63. Peskin, A. V., and Winterbourn, C. C. (2001) Kinetics of the reactions of hypochlorous acid and amino acid chloramines with thiols, methionine, and ascorbate, *Free Radical Biol. Med. 30*, 572−579.
64. Mansoor, M. A., Svardal, A. M., and Ueland, P. M. (1992) Determination of the in vivo redox status of cysteine, cysteinylglycine, homocysteine, and glutathione in human plasma, *Anal. Biochem. 200*, 218−229.
65. Andersson, A., Isaksson, A., Brattstrom, L., and Hultberg, B. (1993) Homocysteine and other thiols determined in plasma by HPLC and thiol-specific postcolumn derivatization, *Clin. Chem. 39*, 1590−1597.
66. Sengupta, S., Chen, H., Togawa, T., DiBello, P. M., Majors, A. K., Budy, B., Ketterer, M. E., and Jacobsen, D. W. (2001) Albumin thiolate anion is an intermediate in the formation of albumin-S-S-homocysteine, *J. Biol. Chem. 276*, 30111−30117.

BI701520Y